The Canadian Journal of Mineralogy and Petrology
ISSN 2817-1713
Vol. 61, pp. 1151-1162 (2023)
DOI: 10.3749/2300041

VIRGILLUETHITE: A NEW MINERAL AND THE NATURAL ANALOGUE OF SYNTHETIC β-$MoO_3 \cdot H_2O$, FROM COOKES PEAK, LUNA COUNTY, NEW MEXICO, USA

HEXIONG YANG[§]

Department of Geosciences, University of Arizona, 1040 E. 4th Street, Tucson, Arizona 85721-0077, USA

XIANGPING GU

School of Geosciences and Info-Physics, Central South University, #932, South Lushan Road, Changsha, Hunan 410083, China

RONALD B. GIBBS AND ROBERT T. DOWNS

Department of Geosciences, University of Arizona, 1040 E. 4th Street, Tucson, Arizona 85721-0077, USA

ABSTRACT

The new mineral virgilluethite, ideally β-$MoO_3 \cdot H_2O$, was discovered in an unnamed short adit on the Summit group of claims near Cookes Peak, Luna County, New Mexico, USA. All virgilluethite crystals are pseudomorphs after sidwillite and occur as aggregates of sub-parallel platy crystals. Associated minerals include sidwillite, raydemarkite, tianhuixinite, ilsemannite, jordisite, powellite, fluorite, baryte, pyrite, and quartz. Virgilluethite is pale yellow-green in transmitted light, transparent with white streak and vitreous luster. It is flexible with a Mohs hardness of ~2; cleavage is perfect on {010}. No twinning was observed visually. The measured and calculated densities are 3.71(5) and 3.69 g/cm^3, respectively. Virgilluethite is insoluble in water or hydrochloric acid. An electron probe microanalysis yielded an empirical formula $(Mo_{1.00})O_3 \cdot H_2O$ based on 4 O *apfu*.

Virgilluethite is the natural analogue of the β-form of $MoO_3 \cdot H_2O$, which was first synthesized over a century ago (Rosenheim & Davidsohn 1903). It is monoclinic, space group $P2_1/c$, with unit-cell parameters $a = 7.2834(3)$, $b = 10.6949(6)$, $c = 7.4861(3)$ Å, $\beta = 112.779(2)°$, $V = 583.03(5)$ Å^3, and $Z = 4$. The crystal structure of virgilluethite, which is topologically identical to that of tungstite ($WO_3 \cdot H_2O$), is characterized by highly distorted and elongated $MoO_5(H_2O)$ octahedra that share four corners in the equatorial plane with one another to form sheets parallel to (010). These sheets, analogous to those in sidwillite, are held together by H-bonding between the H_2O molecule and the O atom in the axial position in the adjacent sheets. Virgilluethite and raydemarkite are dimorphs of $MoO_3 \cdot H_2O$. Unlike virgilluethite, the MoO_6 octahedra in raydemarkite share edges to form isolated double chains, resembling those found in zhenruite, $(MoO_3)_2 \cdot H_2O$.

Keywords: virgilluethite, β-$MoO_3 \cdot H_2O$, molybdenum trioxide hydrates, crystal structure, X-ray diffraction, Cookes Peak.

INTRODUCTION

The new mineral virgilluethite, ideally $MoO_3 \cdot H_2O$, was discovered in an unnamed short adit of the Summit group of claims, near Cookes Peak, Luna County, New Mexico, USA. The new mineral is named in honor of Dr. Virgil W. Lueth, a mineralogist emeritus from the New Mexico Bureau of Geology and Mineral Resources (NMBGMR). Dr. Lueth received his B.S. in geology at the University of Wisconsin and M.S. and Ph.D. degrees from the University of Texas at El Paso. Prior to arriving at NMBGMR, he was a professor of geology at Tarleton State University (Texas A&M System). Dr. Lueth has served on the Board of Directors of the Society of Mineral Museum Professionals, New Mexico Geological Society, New Mexico Geological Society Foundation, and the Friends of Mineralogy. He is also an adjunct curator at the New Mexico Museum

§ *Corresponding author e-mail address*: hyang@arizona.edu

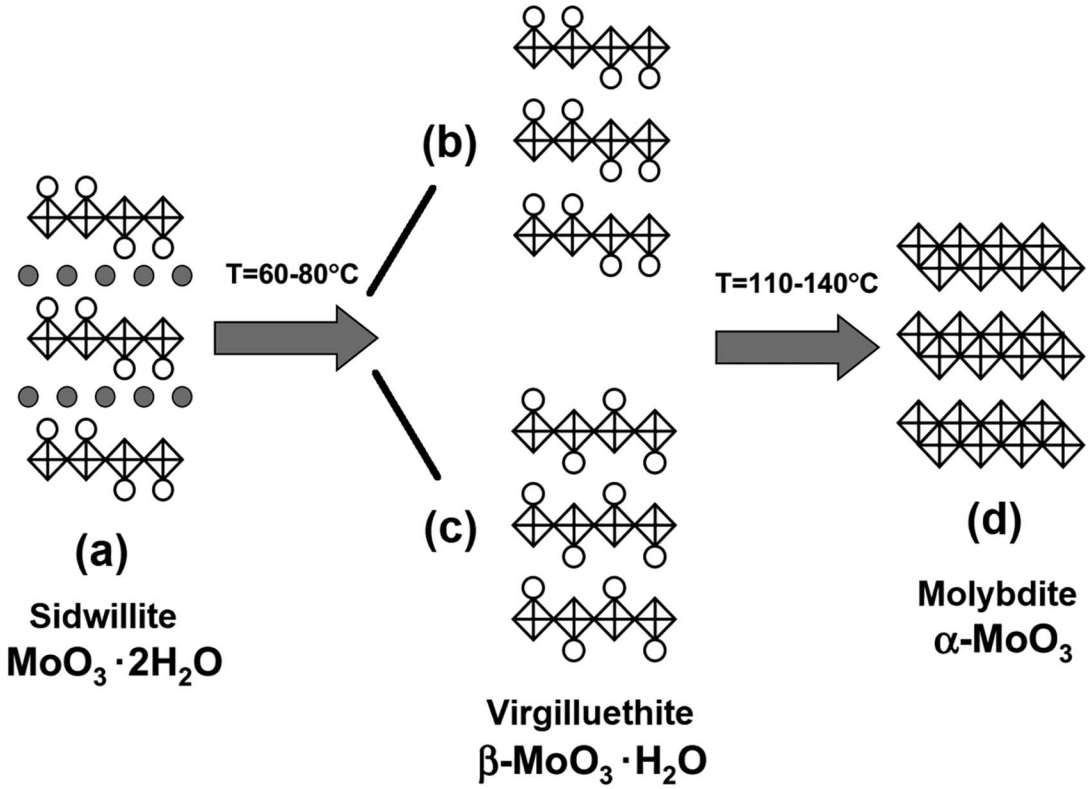

FIG. 1. A schematic view of the crystal structures of (a) sidwillite ($MoO_3 \cdot 2H_2O$) (Krebs 1972, Cesbron & Ginderow 1985), (b, c) virgilluethite (β-$MoO_3 \cdot H_2O$) [(b) Günter 1972, (c) Boudjada *et al*. 1993], and (d) molybdite (α-MoO_3) (Kihlborg 1963, Sitepu 2009). Open circles denote coordinated water molecules, whereas solid circles denote crystal water molecules. The *T* ranges for the two dehydration processes are also presented [after Kuzmin & Purans (2000)].

of Natural History and Science and an adjunct professor of geology at New Mexico Tech. Dr. Lueth was the recipient of the Honorary Award from the Rocky Mountain Federation of Mineral Societies in 1996 for his service to the mineralogical community. He was also named an honorary member of the New Mexico Geological Society in 2005. Dr. Lueth has published over 80 articles in scientific journals, textbooks, and popular magazines, mainly in the fields of mineralogy, geochemistry, and economic geology. He has overseen three iterations of the NMBGMR-New Mexico Tech Mineral Museum and hosted the New Mexico Mineral Symposium annually in November. Before his retirement in 2021, Dr. Lueth held the position of Sr. Mineralogist/Economic Geologist and Director of the Mineral Museum at NMBGMR, where he worked since 1994. The new mineral and its name have been approved by the Commission on New Minerals, Nomenclature and Classification (CNMNC) of IMA (IMA 2023-006). Part of the cotype samples have been deposited at the University of Arizona Alfie Norville Gem and Mineral Museum (Catalogue # 22723) and the RRUFF Project (deposition #R220017) (http://rruff.info).

Molybdenum trioxide (MoO_3) and its related hydrates, namely molybdic acids, ($MoO_3 \cdot nH_2O$, $n = 2$, 1, 1/2, and 1/3) have been an interesting research subject for over a century owing to their versatile applications in electronics, catalysis, sensors, energy-storage units, field-emission devices, lubricants, super-conductors, thermal materials, biosystems, chromogenics, and electrochromic systems (see a thorough review by de Castro *et al*. 2017 and references therein). Thus far, five polymorphs of MoO_3 have been reported. In addition to the orthorhombic (space group *Pbnm*) α-form (Bräkken 1931, Wooster 1931, Andersson & Magléni 1950, Kihlborg 1964, Sitepu 2009), which has been found in nature and named as molybdite (Čech & Povondra 1963), there are four other metastable polymorphs, including both the monoclinic β-MoO_3 and β'-MoO_3 modifications, which have the 3D ReO_3 structure (McCarron

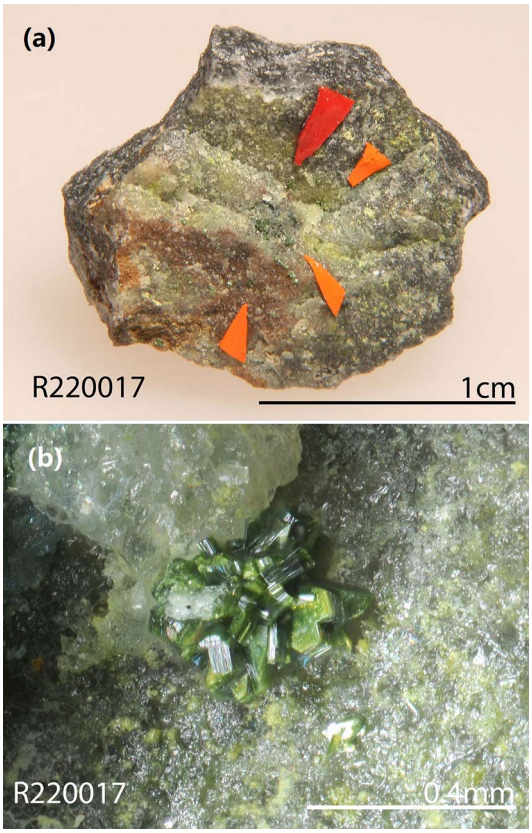

FIG. 2. (a) The specimen on which the new mineral virgilluethite was found. (b) A microscopic view of aggregates of yellowish green platy crystals of virgilluethite on a quartz matrix.

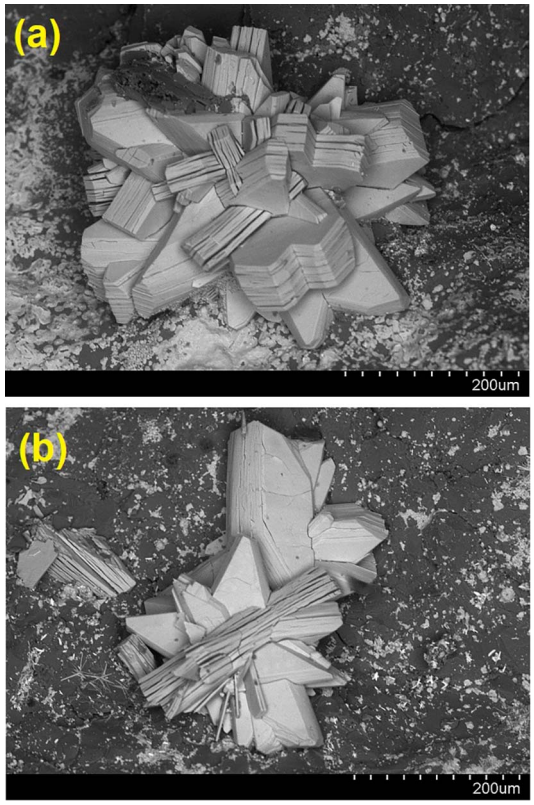

FIG. 3. Two backscattered electron images, showing platy AQ: 1 aggregates of virgilluethite.

1986, Parise *et al*. 1991, Mougin *et al*. 2000, Liu *et al*. 2009); the high-*P* monoclinic ($P2_1/m$) MoO_3-II phase (McCarron & Calabrese 1991); and the hexagonal ($P6_3/m$ or $P6_3$) *h*-MoO_3 phase (Guo *et al*. 1994). For molybdenum trioxide hydrates, six different phases have been documented, including: (1) monoclinic $P2_1/n$ dihydrate $MoO_3 \cdot 2H_2O$ (Krebs 1972, Cesbron & Ginderow 1985), (2) monoclinic $P2/m$ yellow dihydrate $MoO_3 \cdot 2H_2O$ (Schultén 1903, Lindqvist 1950), (3) triclinic $P\bar{1}$ white monohydrate α-$MoO_3 \cdot H_2O$ (Rosenheim & Davidsohn 1903, Böschen & Krebs 1974, Oswald *et al*. 1975), (4) monoclinic $P2_1/c$ yellow monohydrate β-$MoO_3 \cdot H_2O$ (Rosenheim & Davidsohn 1903, Günter 1972, Boudjada *et al*. 1993), (5) monoclinic $P2_1/m$ hemihydrate $MoO_3 \cdot 1/2H_2O$ (Fellows *et al*. 1983, Bénard *et al*. 1994), and (6) hexagonal $P6_3/m$ $MoO_3 \cdot 1/3H_2O$ (Fu *et al*. 2005, Deki *et al*. 2009, Zhao *et al*. 2009, Lunk *et al*. 2010). Among these six hydrated $MoO_3 \cdot nH_2O$ phases, five have been discovered in nature: sidwillite, $MoO_3 \cdot 2H_2O$ (Cesbron & Ginderow 1985); raydemarkite, α-$MoO_3 \cdot H_2O$ (Yang *et al*. 2023); virgilluethite, β-$MoO_3 \cdot H_2O$ (this study); zhenruite, $(MoO_3)_2 \cdot H_2O$ (or $MoO_3 \cdot 1/2H_2O$) (Gu *et al*. 2022a); and tianhuixinite, $(MoO_3)_3 \cdot H_2O$ (or $MoO_3 \cdot 1/3H_2O$) (Gu *et al*. 2022b).

Virgilluethite is the natural analogue of β-$MoO_3 \cdot H_2O$, which was first synthesized over a century ago by Rosenheim & Davidsohn (1903), who also synthesized the α-phase. The α-phase, known as raydemarkite, has been discovered from the same locality as virgilluethite (Yang *et al*. 2023). However, despite its long history, the crystal structure of the β-$MoO_3 \cdot H_2O$ phase has never been fully determined, primarily due to the difficulty in finding crystals suitable for crystal-structure determination. Using powder X-ray diffraction and Weissenberg and precession photography, Günter (1972) found that the dehydration of sidwillite to the β-phase is strongly topotactic with the loss of only interlayer H_2O molecules. Accordingly, Günter (1972) proposed a crystal-structure model for the β-phase (Fig. 1b) based on the measured unit-cell

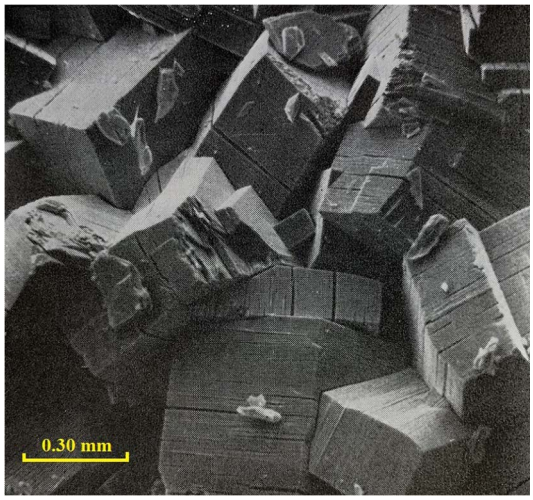

FIG. 4. A backscattered electron image taken from Günter (1972) showing aggregates of sub-parallel plates of synthetic β-phase or virgilluethite after dehydration of sidwillite.

parameters and the proposed space group $P2_1/c$. From a neutron powder thermodiffractometric study, Boudjada *et al*. (1993) confirmed the topotactic character of the dehydration process involving sidwillite but arrived at a crystal-structure model for the β-phase (Fig. 1c) that differed from that proposed by Günter (1972). Boudjada *et al*. (1993) were unable to perform a full crystal-structure refinement due to there being "too many parameters and small angular range of diffraction patterns". This paper describes the physical and chemical properties of virgilluethite and its crystal structure determined from single-crystal X-ray diffraction data, along with elucidating its structural relationships with other hydrated $MoO_3 \cdot nH_2O$ phases.

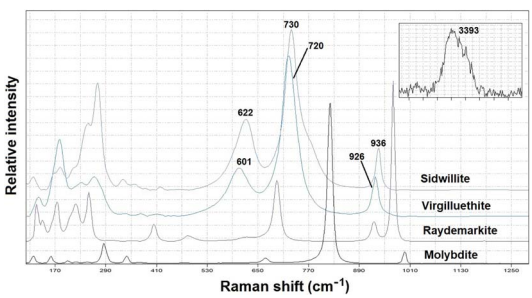

FIG. 5. Raman spectra of molybdite, sidwillite, raydemarkite, and virgilluethite. The inserted figure shows the weak band centered at 3393 cm^{-1} for virgilluethite.

TABLE 1. X-RAY POWDER DIFFRACTION DATA (d in Å, I in %) FOR VIRGILLUETHITE

h	k	l	I_{cal}	I_{meas}	d_{cal}	d_{meas}
0	**2**	**0**	**100.0**	**62**	**5.350**	**5.346**
1	1	1	4.1	5	4.653	4.643
$\overline{1}$	2	1	10.3	7	3.757	3.760
0	**1**	**2**	**78.6**	**90**	**3.533**	**3.531**
2	**1**	**0**	**82.2**	**100**	**3.448**	**3.445**
1	**3**	**1**	**12.2**	**8**	**2.935**	**2.938**
0	**4**	**0**	**15.0**	**26**	**2.675**	**2.654**
2	**0**	**2**	**9.6**	**19**	**2.584**	**2.587**
$\overline{1}$	4	1	10.3	8	2.386	2.379
2	2	2	4.7	2	2.327	2.331
1	2	3	1.7	2	2.148	2.158
1	5	1	6.9	6	1.977	1.978
$\overline{3}$	3	1	2.9	1	1.947	1.948
0	**0**	**4**	**6.2**	**11**	**1.872**	**1.865**
4	0	0	8.0	4	1.821	1.822
1	1	4	2.1	7	1.779	1.772
4	2	0	7.3	5	1.724	1.725
$\overline{1}$	6	1	4.7	2	1.689	1.691
2	1	$\overline{4}$	3.9	2	1.659	1.661
$\overline{4}$	1	2	5.3	8	1.632	1.632
4	1	2	4.4	1	1.606	1.607
$\overline{3}$	5	1	2.8	1	1.574	1.572
0	4	4	2.0	2	1.533	1.537
4	4	0	2.9	5	1.505	1.501
4	3	2	2.1	2	1.478	1.479
1	7	1	3.2	4	1.466	1.468
1	6	3	1.8	2	1.420	1.418
3	6	1	2.3	2	1.408	1.410
4	0	$\overline{4}$	1.3	2	1.319	1.320
$\overline{4}$	5	2	1.0	1	1.307	1.307
$\overline{1}$	8	1	2.0	2	1.296	1.295
$\overline{3}$	7	1	1.7	1	1.277	1.279
6	1	0	1.4	1	1.206	1.206
1	9	1	1.2	4	1.159	1.159

SAMPLE DESCRIPTION AND EXPERIMENTAL METHODS

Occurrence, physical and chemical properties, and Raman spectra

Virgilluethite was found on a specimen (Fig. 2a) collected by Mr. Ray Demark on February 18, 2016, in an unnamed short adit of the Summit group of claims (32° 33' 47" N and 107° 43' 48" W) near Cookes Peak, at the southern end of the Cookes Range, Luna County, New Mexico, USA. All virgilluethite crystals are pseudomorphs after sidwillite, apparently resulting from the topotactic dehydration (loss of interlayer H_2O molecules) of sidwillite (Günter 1972, Boudjada *et al*. 1993). All crystals of virgilluethite >10 μm in length

TABLE 2. COMPARISON OF CRYSTALLOGRAPHIC DATA FOR VIRGILLUETHITE

	Virgilluethite Natural	Virgilluethite Synthetic	Virgilluethite Synthetic
Ideal formula	$MoO_3 \cdot H_2O$	$MoO_3 \cdot H_2O$	$MoO_3 \cdot H_2O$
Crystal symmetry	Monoclinic	Monoclinic	Monoclinic
Space group	$P2_1/c$	$P2_1/c$	$P2_1/c$
a (Å)	7.2834(3)	7.55	7.548
b (Å)	10.6949(6)	10.69	10.712
c (Å)	7.4861(3)	7.28	7.237
β (°)	91.084(4)	91	90.77
V (Å^3)	583.03(5)	587.48	585.09
T (°C)	room *T*	80	60–80
Z	4	4	4
ρ_{cal}(g/cm^3)	3.69		
2θ range for data collection (°)	≤130.00 (Cu*K*α)		
No. of reflections collected	5489		
No. of independent reflections	999		
No. of reflections with $I > 2\sigma(I)$	955		
No. of parameters refined	94		
R(int)	0.056		
Final R_1, wR_2 factors [$I > 2\sigma(I)$]	0.075, 0.189		
Goodness-of-fit	1.115		
Measurement method	Single-crystal X-ray diffraction	Weissenberg & Precession	Neutron Powder diffraction
References	(1)	(2)	(3)

References: (1) This study, (2) Günter (1972), (3) Boudjada *et al.* (1993).
Note: Although all three data sets have the same space group, our *a* and *c* parameters are switched compared to those previously reported.

occur as aggregates of sub-parallel plates (Figs. 2b and 3). This morphology is consistent with that of β-$MoO_3 \cdot H_2O$ formed by dehydration of sidwillite (Fig. 4), as noted by Günter (1972). Furthermore, some aggregates are also intergrowths of virgilluethite and tianhuixinite (Gu *et al*. 2022b). Associated minerals are sidwillite, raydemarkite, tianhuixinite, ilsemannite, jordisite, powellite, fluorite, baryte, pyrite, and quartz.

The Summit group of claims consists of a number of adits, shafts, pits, and trenches, many of which are rich in fluorite. Hydrothermal solutions originating from a granodiorite produced ore bodies localized in limestone units beneath impermeable shales which were subsequently accompanied by silicification, the latter leading to the formation of jasperoids. The Summit group was one of the largest lead, zinc, and silver producers in the

TABLE 3. FRACTIONAL ATOM COORDINATES AND EQUIVALENT ISOTROPIC DISPLACEMENT PARAMETERS (Å^2) FOR VIRGILLUETHITE

Atom	*x/a*	*y/b*	*z/c*	U_{eq}
Mo1	0.63174 (19)	0.22224 (12)	0.34118 (18)	0.0219 (5)
Mo2	0.13146 (19)	0.28163 (12)	0.39858 (17)	0.0211 (5)
O1	0.5900 (17)	0.0677 (12)	0.3319 (15)	0.028 (3)
O2	0.629 (3)	0.262 (2)	0.1163 (16)	0.068 (6)
O3	0.3760 (19)	0.2773 (11)	0.376 (3)	0.062 (7)
O4	0.669 (2)	0.4363 (13)	0.4017 (16)	0.033 (3)
O5	0.0874 (17)	0.4329 (11)	0.3511 (16)	0.027 (3)
O6	0.124 (3)	0.2801 (11)	0.6350 (19)	0.045 (5)
O7	0.8762 (19)	0.2209 (11)	0.378 (3)	0.064 (7)
O8	0.1707 (18)	0.0644 (12)	0.4253 (17)	0.028 (3)

TABLE 4. ATOMIC DISPLACEMENT PARAMETERS (Å^2) FOR VIRGILLUETHITE

Atom	U^{11}	U^{22}	U^{33}	U^{12}	U^{13}	U^{23}
Mo1	0.0156 (8)	0.0305 (9)	0.0196 (7)	−0.0008 (5)	−0.0018 (5)	−0.0027 (5)
Mo2	0.0149 (8)	0.0260 (8)	0.0222 (8)	−0.0006 (5)	−0.0013 (6)	0.0032 (5)
O1	0.022 (6)	0.040 (7)	0.021 (6)	0.016 (5)	−0.004 (5)	0.008 (5)
O2	0.11 (2)	0.082 (13)	0.007 (6)	−0.007 (12)	−0.005 (9)	0.004 (7)
O3	0.018 (8)	0.011 (8)	0.16 (2)	0.007 (5)	0.020 (11)	0.006 (8)
O4	0.040 (8)	0.038 (7)	0.021 (6)	−0.012 (6)	−0.024 (5)	0.004 (5)
O5	0.026 (6)	0.024 (6)	0.032 (6)	−0.010 (5)	0.005 (5)	−0.020 (5)
O6	0.084 (14)	0.012 (7)	0.040 (9)	−0.010 (7)	−0.011 (9)	−0.005 (5)
O7	0.016 (8)	0.011 (8)	0.17 (2)	−0.010 (5)	0.007 (11)	−0.012 (8)
O8	0.025 (6)	0.027 (6)	0.033 (6)	0.008 (5)	−0.009 (5)	0.005 (5)

district (McLemore *et al*. 2001). The upper levels of the mines were highly oxidized and have been completely mined out. A more detailed summary of the geology and mineralogy of Cookes Peak mining district is presented by Simmons (2019).

Virgilluethite is pale yellow-green in transmitted light, transparent with white streak and vitreous luster. It is flexible with a Mohs hardness of ~2; cleavage is perfect on {010}. No twinning was observed visually. The measured (by flotation in heavy liquids) and calculated densities are 3.71(5) and 3.69 g/cm^3, respectively. No optical data were measured because the indices of refraction are too high for measurement with available index liquids. The calculated average index of refraction is 1.92 for the empirical formula based on the Gladstone-Dale relationship (Mandarino 1981). Virgilluethite is insoluble in water or hydrochloric acid.

The chemical composition of virgilluethite was determined with a Shimadzu-1720 electron microprobe operated at 15 keV and 10 nA with a beam size of 1 μm. Pure Mo-metal was used as the standard for Mo. No other elements were detected by EDS. The average of six analytical points gives (wt.%) MoO_3 = 87.07(1.19).

TABLE 5. SELECTED BOND DISTANCES (Å) FOR VIRGILLUETHITE

Virgilluethite (β-MoO_3·H_2O)		Raydemarkite (α-MoO_3·H_2O)	
Mo1–O1	1.681 (14)	Mo–O1	1.6929(14)
–O2	1.737 (13)	–O3	1.6943(14)
–O7	1.796 (14)	–O2	1.9577(10)
–O3	1.975 (13)	–O2’	1.9585(10)
–O2’	2.067 (12)	–O2	2.2671(12)
–O4	2.348 (14)	–O4	2.3286(15)
<*M*–O>	1.934	<*M*–O>	1.9833
OV	9.255		9.703
OAV	93.84		159.57
OQE	1.042		1.064
Mo2–O5	1.686 (13)		
–O6	1.772 (14)		
–O3	1.793 (13)		
–O7	1.973 (13)		
–O6’	2.080 (14)		
–O8	2.349 (12)		
<*M*–O>	1.942		
OV	9.395		
OAV	88.80		
OQE	1.040		
Reference	This study		Yang *et al.* (2023)

Note: OV = Octahedral volume, OAV = Octahedral angle variance, OQE = Octahedral quadratic elongation (Robinson *et al.* 1971).

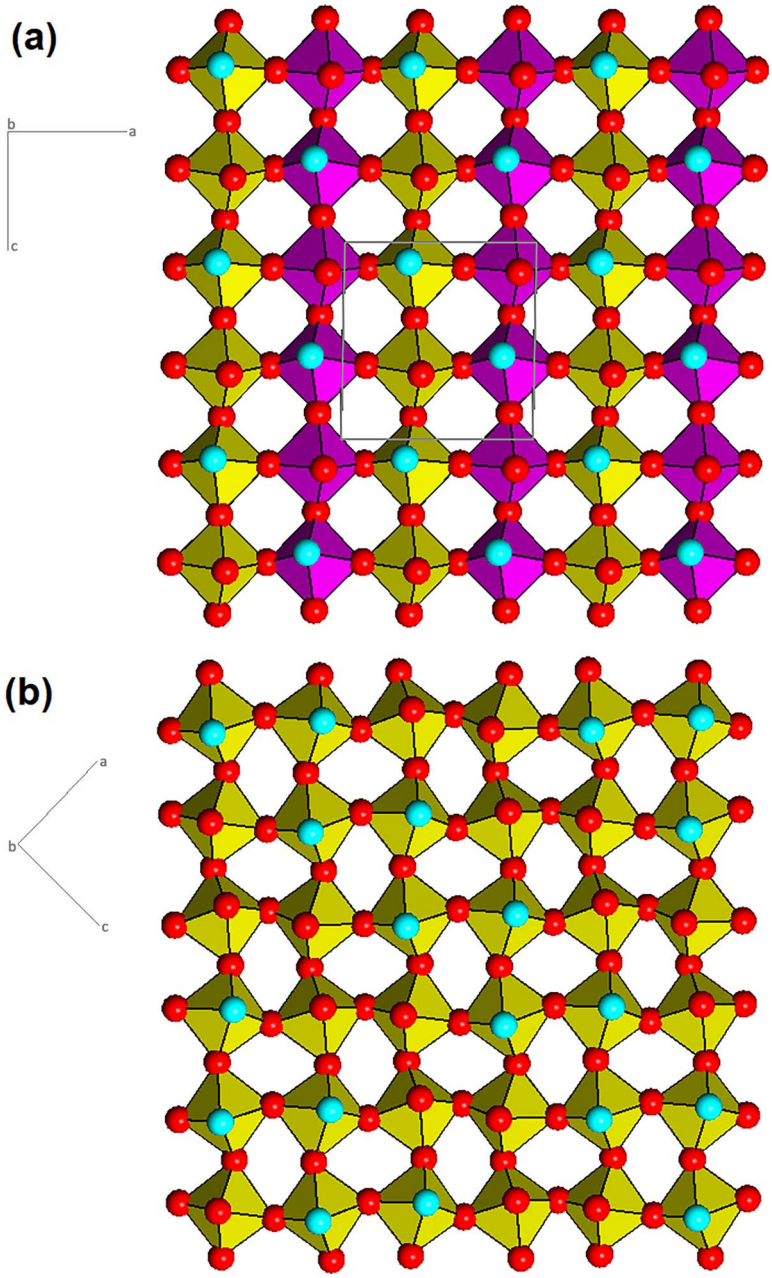

FIG. 6. A comparison of the crystal structures of (a) virgilluethite and (b) sidwillite, showing a corner-shared $MoO_5(H_2O)$ octahedral layer parallel to [010]. For virgilluethite, yellow and purple octahedra represent $Mo1O_5(H_2O)$ and $Mo2O_5(H_2O)$ groups, respectively. Red and aqua spheres represent O atoms and H_2O molecules, respectively.

The chemical formula was calculated on the basis of 4 O *apfu*, as determined from the structure refinement, by adding 11.05 wt.% H_2O as the ideal value, yielding an empirical formula $(Mo_{1.00})O_3 \cdot H_2O$.

The Raman spectrum (Fig. 5) of virgilluethite was collected from a randomly oriented crystal on a Thermo Almega microRaman system using a solid-state laser with $\lambda = 532$ nm and a thermoelectric

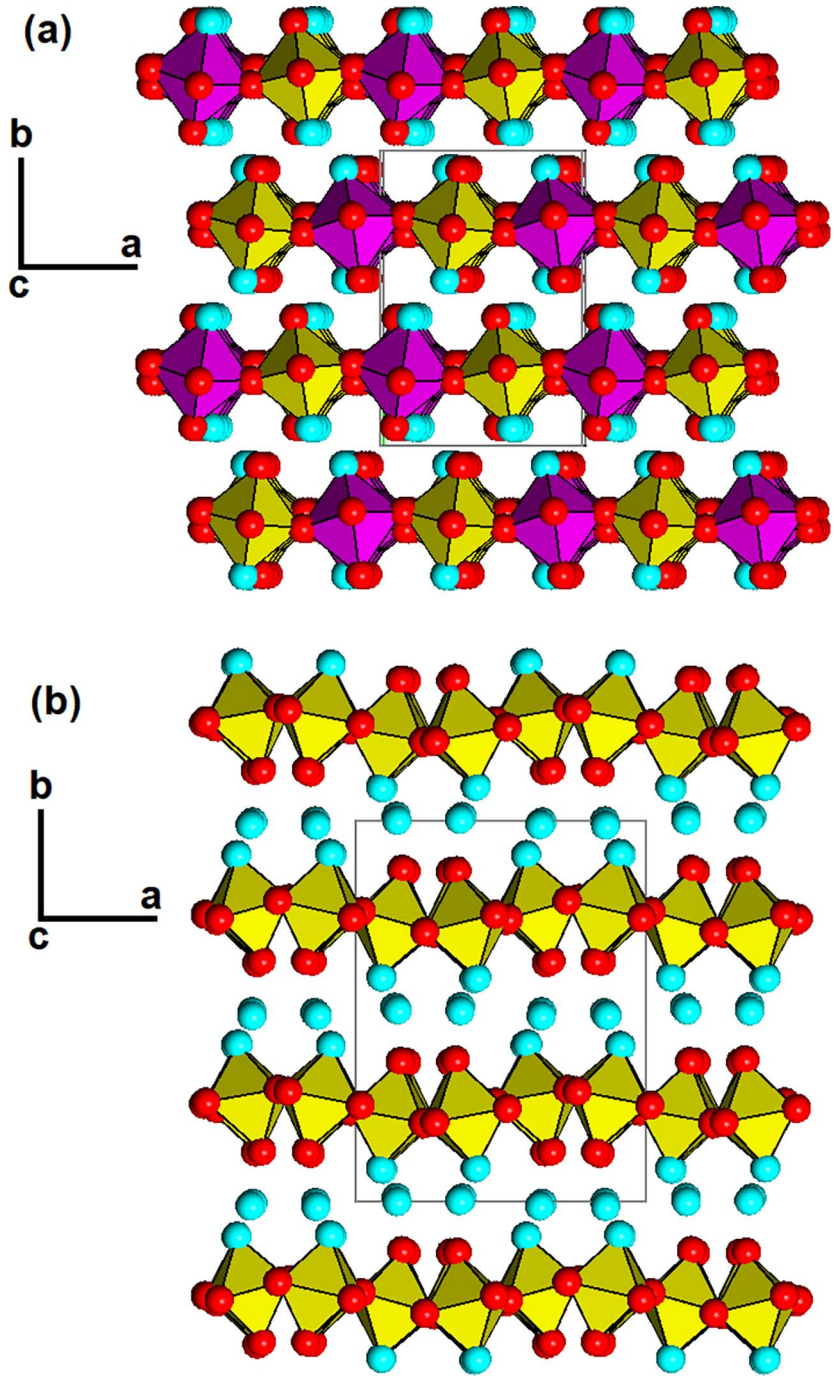

FIG. 7. A comparison of the crystal structures of (a) virgilluethite and (b) sidwillite, showing the stacking of the $MoO_5(H_2O)$ octahedral layers along [010]. The figure legends are the same as in Figure 6.

TABLE 6. BOND-VALENCE SUMS FOR VIRGILLUETHITE

Atom	Mo1	Mo2	Sum
O1	1.767		1.767
O2	1.545		2.236
	0.691		
O3	0.864	1.346	2.210
O4	0.347		0.347
O5		1.749	1.749
O6		1.418	2.086
		0.668	
O7	1.337	0.868	2.205
O8		0.347	0.347
Sum	6.551	6.396	

cooled CCD detector. The laser is partially polarized with 4 cm^{-1} resolution and has a spot size of 1 μm. For comparison, the Raman spectra of molybdite (MoO_3), sidwillite ($MoO_3 \cdot 2H_2O$), and raydemarkite ($MoO_3 \cdot H_2O$) from the RRUFF Project (http://rruff.info/R210024, http://rruff.info/R210025, and http://rruff.info/R210023, respectively) are also plotted in Figure 5. A resemblance between the Raman spectra of virgilluethite and sidwillite is evident, except relative shifts in some peak positions, indicating similarities in their crystal structures. The major band assignments are discussed below.

X-ray crystallography

Both the powder and single-crystal X-ray diffraction data for virgilluethite were collected on a Rigaku Xtalab Synerg D/S 4-circle diffractometer equipped with Cu$K\alpha$ radiation ($\lambda = 1.54184$ Å). Powder X-ray diffraction data were collected in the Gandolfi mode at 50 kV and 1 mA (Table 1), and the unit-cell parameters refined using the program by Holland & Redfern (1997) are $a = 7.2870(2)$, $b = 10.6991(3)$, $c = 7.4877(3)$ Å, $\beta = 91.198(4)°$, and $V = 583.64(3)$ $Å^3$.

All virgilluethite crystals occur as aggregates of multi sub-parallel plates. This is suggested by the occurrence of relatively large, diffuse diffraction spots with streaks, and this likely explains the relatively large R_1 factor (0.075) and the abnormal displacement parameters for some O atoms (O2, O3, and O7). The existence of broadened reflections of β-$MoO_3 \cdot H_2O$ formed through dehydration of sidwillite was also observed by Günter (1972) in data from Weissenberg and precession photographs. Examination of systematic absences in this current study suggests the unique space group $P2_1/c$. The crystal structure was solved using SHELXT (Sheldrick 2015a) and refined using SHELXL2019 (Sheldrick 2015b). No H atoms were located through examination of the difference Fourier syntheses. The refinement statistics are given in Table 2. Final atomic coordinates and displacement parameters for virgilluethite are given in Tables 3 and 4, respectively. Selected bond distances are presented in Table 5[1].

It is worth noting that although all three data sets listed in Table 2 have the same space group, $P2_1/c$, our unit-cell parameters a and c ($a < c$) are reversed compared to those (*i.e.*, $a > c$) reported by Günter (1972) and Boudjada *et al*. (1993). If the unit-cell setting with $a > c$ is adopted, then the correct space group is $P2_1/a$. It is unclear whether the reversal in a and c as is done herein is related to the kinetics of dehydration process, as both Günter (1972) and Boudjada *et al*. (1993) obtained synthetic virgilluethite by dehydration of sidwillite between 60 and 80° C in only a few hours.

Discussion

Crystal structure

The crystal structure of virgilluethite determined in this study confirms the model proposed by Boudjada *et al*. (1993). It is characterized by highly distorted and elongated (along [100]) $MoO_5(H_2O)$ octahedra, which share four corners in the equatorial plane with one another to form sheets parallel to (010) (Fig. 6a). These sheets are topologically identical to those in sidwillite (Fig. 6b). The sheets of octahedra are held together by H-bonding between the H_2O molecules and the O atoms in the axial position in the adjacent sheets (Fig. 7a). By comparison, the sheets of octahedra in sidwillite are instead joined together by interlayer H_2O molecules (Fig. 7b). In particular, Figure 6a illustrates that H_2O molecules in virgilluethite alternate on the axial corners of $MoO_5(H_2O)$ octahedra along [101]. Such an arrangement of H_2O molecules is evidently different from that in sidwillite (Fig. 6b), implying that the dehydration of sidwillite to virgilluethite does not simply involve removal of interlayer H_2O molecules, followed by a reduction in the distance between sheets of $MoO_5(H_2O)$ octahedra, as was proposed by Günter (1972) (Fig. 1). It is interesting to note that the crystal structure of virgilluethite is topologically identical to that of tungstite, $WO_3 \cdot H_2O$ (Szymanski & Roberts 1984). Nonetheless, tungstite is orthorhombic with space group *Pmnb*, while virgilluethite is monoclinic with space group $P2_1/c$.

There are two distinct $MoO_5(H_2O)$ octahedra in the virgilluethite crystal structure and both are

[1] Supplementary Data are available from the Depository of Unpublished Data on the MAC website (http://mineralogicalassociation.ca/), document "Virgilluethite, CM 61, 23-00041"

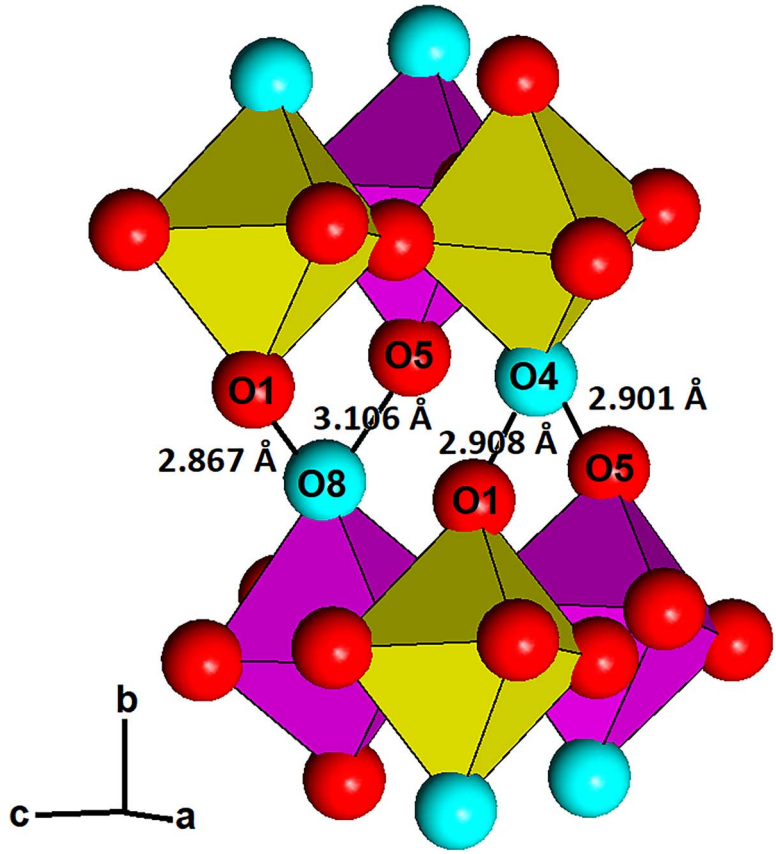

FIG. 8. Hydrogen bonding scheme between two $MoO_5(H_2O)$ octahedral layers in virgilluethite. The figure legends are the same as in Figure 7.

appreciably distorted in a similar fashion, with three short Mo–O bonds between 1.68 and 1.80 Å, two medium Mo–O bonds between 1.97 and 2.10 Å, and one long Mo–O (H_2O) distance of 2.35 Å (Table 5). Similar highly distorted octahedra have also been observed in other Mo-bearing materials, such as molybdite, MoO_3 (Kihlborg 1963, Sitepu 2009); sidwillite, $MoO_3 \cdot 2H_2O$ (Krebs 1972, Cesbron & Ginderow 1985); zhenruite, $(MoO_3)_2 \cdot H_2O$ (Bénard *et al*. 1994, Gu *et al*. 2022a); and raydemarkite (Böschen & Krebs 1974, Oswald *et al*. 1975, Yang *et al*. 2023).

Raman spectra

According to the Raman spectroscopic studies on $MoO_3 \cdot H_2O$ and $MoO_3 \cdot 2H_2O$ (Saleem & Aruldhas 1983, Seguin *et al.* 1995, Chandra *et al.* 1987, Oyerinde *et al*. 2008, Yang *et al*. 2023), tentative assignments of major Raman bands for virgilluethite were made. The weak band centered at 3393 cm^{-1} is assigned to the O–H stretching vibrations. The bands at 720 cm^{-1} and the weak band at 926 cm^{-1} are attributed to the Mo–O symmetric and antisymmetric stretching vibrations within the MoO_6 group, respectively. The bands between 370 and 700 cm^{-1} are ascribable to the O–Mo–O bending modes within the MoO_6 group. The bands below 350 cm^{-1} are mainly associated with the rotational and translational modes of MoO_6 and H_2O groups, as well as the lattice vibrational modes.

The bond-valence calculations using the parameters given by Brown (2009) (Table 6) indicate that O4 and O8 are H_2O molecules. The deficiencies in the bond valences for O1 and O5 are compensated by the hydrogen bonds, as both of them are engaged in the hydrogen bonding as acceptors: O4···O1 = 2.901 Å, O4···O5 = 2.908 Å, O8···O1 = 2.867 Å, and O8···O5 = 3.106 Å (Fig. 8). According to the correlation between O–H stretching frequencies (ν_{O-H}) and O–H···O distances for minerals (Libowitzky 1999), the weak Raman band centered at 3393 cm^{-1} corresponds well with the O–O distances between 2.85 and 3.10 Å.

Virgilluethite and raydemarkite are dimorphs of $MoO_3 \cdot H_2O$ and are termed as the β- and α-forms in the literature, respectively. Unlike raydemarkite, in which the MoO_6 octahedra share edges to form isolated double chains (Böschen & Krebs 1974, Oswald *et al*. 1975, Yang *et al.* 2023), the MoO_6 octahedra in virgilluethite share corners to form layers, similar to those in molybdite (Kihlborg 1963, Sitepu 2009) and sidwillite (Krebs 1972, Cesbron & Ginderow 1985). Therefore, it is conceivable that, relative to raydemarkite, virgilluethite is energetically favored to form through the dehydration of sidwillite. In fact, Günter (1972) and Boudjada *et al*. (1993) have demonstrated that synthetic sidwillite dehydrates readily to form synthetic virgilluethite between 60 and 80 °C through a topotactic mechanism (Table 2). The structural difference between raydemarkite and virgilluethite may also provide the explanation as to why both minerals can be synthesized from the chemical reactions in solutions, but only virgilluethite can be obtained by dehydration of sidwillite. Thus far, there is no report of the formation of raydemarkite through the dehydration of sidwillite. Nevertheless, both raydemarkite and virgilluethite will dehydrate to become molybdite, MoO_3, upon heating between 110 and 160 °C (Günter 1972, Oswald *et al*. 1975, Boudjada *et al*. 1993).

Acknowledgments

This study was supported by the Feinglos family. We are grateful to Dr. John Hughes for the constructive comments.

References

Andersson, G. & Magnéli, A. (1950) On the crystal structure of molybdenum trioxide. *Acta Chemica Scandinavica* **4**, 793–797.

Bénard, P., Sequin, L., Louër, D., & Figlarz, M. (1994) Structure of MoO3·1/2H2O by conventional X-ray powder diffraction. *Journal of Solid State Chemistry* **108**, 170–176.

Böschen, V.I. & Krebs, B. (1974) Kristallstruktur der 'weissen molybdänsäure' α-$MoO_3.H_2O$. *Acta Crystallographica* **B30**, 1795–1800.

Boudjada, N., Rodriguez-Carvajal, J., Anne, M., & Figlarz, M. (1993) Dehydration of $MoO_3 \cdot 2H_2O$: A neutron thermodiffractometry study. *Journal of Solid State Chemistry* **105**, 211–222.

Bräkken, H. (1931) Die kristallstrukturen der trioxyde von chrom, molybdän und wolfram. *Zeitschrift für Kristallographie* **78**, 484–488.

Brown, I.D. (2009) Recent developments in the methods and applications of the bond valence model. *Chemical Reviews* **109**, 6858–6919.

Čech, F. & Povondra, P. (1963) Natural occurrence of molybdenum trioxide, MoO_3, in Krupka (Molybdite, a new mineral). *Acta Universitatis Carolinae - Geologica* **1**, 1–14.

Cesbron, F. & Ginderow, D. (1985) La sidwillite, $MoO_3 \cdot 2H_2O$; une nouvelle espèce minérale de Lake Como, Colorado, U.S.A. *Bulletin de Minéralogie* **108**, 813–823 (in French with English abstract).

Chandra, S., Singh, N., Singh, B., Verma, A.L., Khatri, S.S., & Chakrabarty, T. (1987) Laser Raman spectral studies under D.C. bias on fast proton transport in molybdic acid ($MoO_3 \cdot 2H_2O$). *Journal of Physical and Chemical Solids* **48**, 1165–1171.

De Castro, I.A., Datta, R.S., Ou, J.Z., Castellanos-Gomez, A., Sriram, S., Daeneke, T., & Kalantar-Zadeh, K. (2017) Molybdenum oxides – From fundamentals to functionality. *Advanced Materials* **28**(40), 1701619. DOI: https://doi.org/10.1002/adma.201701619

Deki, S., Béléké, A.B., Kotani, Y., & Mizuhata, M. (2009) Liquid phase deposition synthesis of hexagonal molybdenum trioxide thin films. *Journal of Solid State Chemistry* **182**, 2362–2367.

Fellows, R.L., Lloyd, M.H., Knight, J.F., & Yakel, H.L. (1983) X-ray diffraction and thermal analysis of molybdenum (VI) oxide hemihydrate: Monoclinic $MoO_3.1/2H_2O$. *Inorganic Chemistry* **22**, 2468–2470.

Fu, G., Xu, X., Lu, X., & Wan, H. (2005) Mechanisms of methane activation and transformation on molybdenum oxide based catalysts. *Journal of the American Chemical Society* **127**, 3989–3996.

Gu, X., Yang, H., & Scott, M.M. (2022a) Zhenruite, IMA2022-050. CNMNC Newsletter. *Mineralogical Magazine*, **86**.

Gu, X., Gibbs, R.B., & Yang, H. (2022b) Tianhuixinite, IMA2022-081. CNMNC Newsletter. *Mineralogical Magazine*, **70**.

Günter, J.R. (1972) Topotactic dehydration of molybdenum trioxide-hydrates. *Journal of Solid State Chemistry* **5**, 354–359.

Guo, J., Zavalij, P., & Whittingham, M.S. (1994) Preparation and characterization of a MoO_3 with hexagonal structure. *European Journal of Solid State and Inorganic Chemistry* **31**, 833–842.

Holland, T.J.B. & Redfern, S.A.T. (1997) Unit cell refinement from powder diffraction data: The use of regression diagnostics. *Mineralogical Magazine* **61**, 65–77.

Kihlborg, L. (1963) Least squares refinement of the crystal structure of molybdenum trioxide. *Arkiv för Kemi* **21**, 357–364.

Krebs, B. (1972) Die kristallstruktur von $MoO_3 \cdot 2H_2O$. *Acta Crystallographica* **B28**, 2222–2231.

Libowitzky, E. (1999) Correlation of O–H stretching frequencies and O–H···O hydrogen bond lengths in minerals. *Monatshefte für Chemie* **130**, 1047–1059.

Lindqvist, I. (1950) The crystal structure of the yellow molybdic acid, $MoO_3 \cdot 2H_2O$. *Acta Chemica Scandinavica* **4**, 650–657.

Liu, D., Lei, W.W., Hao, J., Liu, D.D., Liu, B.B., Wang, X., Chen, X.H., Cui, Q.L., Zou, G.T., Liu, J., & Jiang, S. (2009) High-pressure Raman scattering and X-ray diffraction of phase transitions in MoO_3. *Journal of Applied Physics* **105**, 023513.

Lunk, H.J., Hartl, H., Hartl, M.A., Fait, M.J., Shenderovich, I.G., Feist, M., Frisk, T.A., Daemen, L.L., Mauder, D., Eckelt, R., & Gurinov, A.A. (2010) "Hexagonal molybdenum trioxide" – known for 100 years and still a fount of new discoveries. *Inorganic Chemistry* **49**, 9400–9408.

Mandarino, J.A. (1981) The Gladstone-Dale relationship. IV. The compatibility concept and its application. *The Canadian Mineralogist* **19**, 441–450.

McCarron, E.M. (1986) β-MoO_3: A metastable analogue of WO_3. *Journal of the Chemical Society*, *Chemical Communications* **1986**, 336.

McCarron, E.M. & Calabrese, J.C. (1991) The growth and single crystal structure of a high pressure phase of molybdenum trioxide: MoO_3-II. *Journal of Solid State Chemistry* **91**, 121–125.

McLemore, V.T., Donahue, K., Breese, M., Jackson, M.L., Arbuckle, J., & Jones, G. (2001) *Mineral Resource Assessment of Luna County, New Mexico*. New Mexico Bureau of Geology and Mineral Resources Open-file Report OF-459, September, 2001, Socorro, New Mexico, USA.

Mougin, O., Dubois, J., & Mathieu, F. (2000) Metastable hexagonal vanadium molybdate study. *Journal of Solid State Chemistry* **152**, 353–360.

Oswald, H.R., Günter, J.R., & Dubler, E. (1975) Topotactic decomposition and crystal structure of white molybdenum trioxide-monohydrate: Prediction of structure by topotaxy. *Journal of Solid State Chemistry* **13**, 330–338.

Oyerinde, O.F., Weeks, C.L., Anbar, A.D., & Spiro, T.G. (2008) Solution structure of molybdic acid from Raman spectroscopy and DFT analysis. *Inorganica Chimica Acta* **361**, 1000–1007.

Parise, J.B., McCarron, E.M., Dreele, R.V., & Goldstone, J. A. (1991) β-MoO_3 produced from a novel freeze drying route. *Journal of Solid State Chemistry* **93**, 193–201.

Robinson, K., Gibbs, G.V., & Ribbe, P.H. (1971) Quadratic elongation: A quantitative measure of distortion in coordination polyhedra. *Science* **172**, 567–570.

Rosenheim, A. & Davidsohn, I. (1903) Die hydrate der molybdänsäure. *Zeitschrift für Anorganische und Allgemeine Chemie* **37**, 314–325 (in German).

Saleem, S.S. & Aruldhas, G. (1983) Vibrational spectra of α-molybdic acid-$MoO_3 \cdot H_2O$. *Pramana* **21**, 283–291.

Schultén, A.B.A. (1903) Recherches sur l'arséniate dicalcique. Reproduction artificielle de la pharmacolite et de la haidingerite. *Bulletin de Minéralogie* **26**, 18–24 (in French).

Seguin, L., Figlarz, M., Cavagnat, R., & Lasskgues, J.-C. (1995) Infrared and Raman spectra of MoO_3, molybdenum trioxides and $MoO_3 \cdot xH_2O$ molybdenum trioxide hydrates. *Spectrochimica Acta, Part A* **51**, 1323–1344.

Sheldrick, G.M. (2015a) SHELXT – Integrated space-group and crystal structure determination. *Acta Crystallographica* **A71**, 3–8.

Sheldrick, G.M. (2015b) Crystal structure refinement with SHELX. *Acta Crystallographica* **C71**, 3–8.

Simmons, P. (2019) Cookes Peak Mining District, Luna County, New Mexico. *Rocks & Minerals* **94**, 214–239.

Sitepu, H. (2009) Texture and structural refinement using neutron diffraction data from molybdite (MoO_3) and calcite ($CaCO_3$) powders and a Ni-rich $Ni_{50.7}Ti_{49.30}$ alloy. *Powder Diffraction* **24**, 315–326.

Szymanski, J.T. & Roberts, A.C. (1984) The crystal structure of tungstite, $WO_3 \cdot H_2O$. *The Canadian Mineralogist* **22**, 681–688.

Wooster, N. (1931) The crystal structure of molybdenum trioxide, MoO_3. *Zeitschrift für Kristallographie* **80**, 504–512.

Yang, H., Gu, X., Sousa, F.X. Gibbs, R.B., McGlasson, J.A., & Downs, R.T. (2023) Raydemarkite, the natural analogue of synthetic α-$MoO_3 \cdot H_2O$, from Cookes Peak, Luna County, New Mexico, USA. *The Canadian Journal of Mineralogy and Petrology* **61**, 203–213.

Zhao, J., Ma, P., Wang, J., & Niu, J. (2009) Synthesis and structural characterization of a novel three-dimensional molybdenum–oxygen framework constructed from Mo_3O_9 units. *Chemistry Letters* **38**, 694–695.

Received June 9, 2023. Revised manuscript accepted July 17, 2023.

This manuscript was handled by Associate Editor Yuanming Pan and Editor Andrew McDonald.